Journal of Biomechanics 88 (2019) 95–103

Contents lists available at ScienceDirect

Journal of Biomechanics

journal homepage: www.elsevier.com/locate/jbiomech
www.JBiomech.com

MRI-based modeling of spleno-mesenteric confluence flow

David R. Rutkowski [a,b,*], Rafael Medero [a,b], Felix J. Garcia [a], Alejandro Roldán-Alzate [a,b,c]

[a] Mechanical Engineering, University of Wisconsin, Madison, WI, United States
[b] Radiology, University of Wisconsin, Madison, WI, United States
[c] Biomedical Engineering, University of Wisconsin, Madison, WI, United States

ARTICLE INFO

Article history:
Accepted 16 March 2019

Keywords:
Portal vein
Hepatic hemodynamics
Helical flow
Cirrhosis
4D flow MRI

ABSTRACT

Characterization of hepatic blood flow magnitude and distribution can lead to a better understanding of the pathophysiology of liver disease. However, the underlying patterns and dynamics of hepatic flow, such as the helical flow structure that often develops following the spleno-mesenteric confluence (SMC) of the hepatic portal vein, have not yet been comprehensively studied. In this study, we used magnetic resonance image (MRI)-based computational models to study the effects of the helical flow structure and SMC geometry on portal blood flow distribution. Additionally, we examined these flow dynamics with four-dimensional (4D) flow MRI in a group of 12 cirrhotic patients and healthy subjects. A validation model was also created to compare computational data to particle image velocimetry (PIV) data. We found significant correlations between flow structure development, vessel geometry, and blood flow distribution in both virtually modified models and in healthy and cirrhotic subjects. However, the direction of these correlations varied among vessel configuration types. Nonetheless, validation model results displayed good qualitative agreement with computational model data.

1. Introduction

Hemodynamic information, such as pressure, flow velocity, and stress, can provide insight into the presence or severity of a variety of hepatic conditions such as portal hypertension, fibrosis, occlusion, and progression of diseases such as hepatocellular carcinoma and cirrhosis (Cohn et al., 1972; Richardson and Withrington, 1981; Scheinfeld et al., 2009; Zhang et al., 2011). Many of these liver diseases are known to have heterogeneous lobar distributions, which have been hypothesized to be a result of imbalanced blood flow distribution between portal venous branches. The blood flow magnitude and distribution can be characterized to provide information on the pathophysiology of liver diseases that affect or depend on the hepatic vasculature (Lara et al., 2011; Roldán-Alzate et al., 2015). However, despite the relevant work focused on flow magnitude and distribution (Cohn et al., 1972; Ralls, 1990; Lara et al., 2011; Zhang et al., 2011; Roldán-Alzate et al., 2016), the underlying patterns and dynamics of blood flow in the hepatic vasculature, and particularly the portal vein (PV), have not yet been comprehensively studied. One particular pattern often observed in portal flow is a helical structure in the main PV branch, directly following the confluence of the splenic vein (SV) and superior mesenteric vein (SMV). Observation of this pattern became feasible with the development of color Doppler sonography, which was used to observe swirling and twisting patterns of hepatopetal flow in the portal venous system by noting alternating bands of color in the portal vessels (Ralls, 1990; Sugimoto et al., 2002). Such work noted that changes in this flow pattern may be particularly prevalent in patients with liver disease. For example, Rosenthal et al. found through Doppler ultrasound that helical flow is unusual in the PV of normal individuals, however, it was observed in approximately 20% of post-transplantation patients and patients with severe liver disease or portosystemic shunts (Rosenthal et al., 1995).

The anatomical structure of the PV may play a significant role in the development of hemodynamic patterns, such as the portal helix. Accordingly, the relationship between PV structure and flow may be of clinical importance. To examine this, Van As et al. studied the anatomical structure of the PV by creating resin casts of the

Abbreviations: IRB, Institutional Review Board; HIPAA, health insurance portability and accountability act; 4D Flow MRI, Four Dimensional Flow Magnetic Resonance Imaging; PC-VIPR, Phase Contrast with Vastly Undersampled Isotropic Projection Reconstruction; DICOM, Digital Imaging and Communications in Medicine; PV, portal vein; SV, Splenic Vein; SMV, superior mesenteric vein; SMC, spleno-mesenteric confluence; CFD, computational fluid dynamics; PIV, particle image velocimetry; LPV, left portal vein; RPV, right portal vein.

* Corresponding author at: A0407 – 1513 University Ave., Madison, WI 53706-1539, United States.
E-mail address: drutkowski2@wisc.edu (D.R. Rutkowski).

https://doi.org/10.1016/j.jbiomech.2019.03.025
0021-9290/

portal venous system of various species (Van As et al., 2001). Through this work, it was found that the portal vein has a unique muscle structure with two perpendicular layers, high mitochondria density, and a rich nerve supply, suggesting that the helical structure may be activated by physiological and pathological conditions (Van As et al., 2001). It has also been observed that helical flow is often transient due to varying metabolic activity, which may support the hypothesis that portal venous activation plays a role in the helical flow pattern (Rosenthal et al., 1995). Structural features of the hepatic vasculature both upstream and downstream of the portal vein may also have a significant influence on portal hemodynamics. Such effects have been studied in the hepatic veins with particle image velocimetry (PIV), showing that orientation of the inlet vessels can have a significant effect on hepatic venous flow distribution (Lara et al., 2011). However, the hemodynamic effects of the orientation of the SMV and SV at the splenomesenteric confluence (SMC) on helical flow development and distal portal blood flow distribution have yet to be determined. If the underlying causes of maldistribution of distal portal blood flow can be determined, then treatment methods may be better informed.

Advanced medical imaging and computational methods have been well established in the study of hepatic hemodynamics. Four-dimensional (4D) flow magnetic resonance (MR) imaging, which offers spatial and temporal flow information that can be used to derive hemodynamic parameters, has emerged as a useful tool in assessment of hepatic vasculature (Roldán-Alzate et al., 2013). In combination with this imaging modality, computational techniques can provide insight into the flow patterns in a variety of anatomical and physiological situations, such as development of the portal helix. For example, Ho et al. observed the development of strong helical flows after the SMC using computational simulation (Ho et al., 2012). Similar helical flow patterns were observed in subsequent work on surgical planning for live donor liver transplantation using computational methods (Rutkowski et al., 2017). However, to establish the reliability of computational and imaging results, fluid dynamic validation methods are still required.

The purpose of this study was to examine the effects of varying SMC confluence anatomy on blood flow distribution and helical flow patterns in the portal vein. To do this, 4D flow MRI data from liver donors was used with computational tools to simulate hemodynamic outcomes from a variety of portal confluence orientations. Additionally, pre- and post-meal 4D flow MRI data from six cirrhotic patients and six healthy volunteers were analyzed to examine the effects of the portal helix flow pattern and SMC geometry on in-vivo portal hemodynamics. Lastly, a validation model was created and analyzed with particle image velocimetry to provide a fluid dynamic comparison between methods.

2. Methods

Human subjects: In this Institutional Review Board approved and Health Insurance Portability and Accountability Act – compliant study, two human subject datasets were used.

Computational Study: Data from a previous study on surgical planning for living donor liver transplantation, was used retrospectively (Rutkowski et al., 2017). Three healthy subjects with no known liver disease, being evaluated for liver donation, were recruited. Written informed consent was obtained prior to inclusion.

In-vivo Study: Data from a study analyzing the effects of a meal challenge on the regulation of portal venous flow was used retrospectively (Roldán-Alzate et al., 2015). Twelve subjects, six with cirrhosis and six with no known liver disease, were recruited. Written informed consent was obtained prior to inclusion.

4D MR Imaging and Analysis: The subjects were imaged on a clinical 3T imaging system (Discovery MR 750, GE Healthcare, Waukesha, WI) with a 32-chanel body coil (NeoCoil, Pewaukee, WI). 4D velocity mapping was achieved using a cardiac-gated time-resolved 3D radially undersampled phase contrast (PC) acquisition (5-point PC-VIPR) (Johnson et al., 2008) with increased velocity sensitivity performance (Zhang et al., 2011; Roldán-Alzate et al., 2013). Acquisition parameters are described in previous work (Rutkowski et al., 2017). The liver transplant donors received 0.05 mmol/kg of gadoxetic acid (Eovist, Bayer Healthcare, Wayne, NJ) approximately 20 min prior to 4D flow MRI. The twelve subjects used for the in-vivo study were imaged both before and after a meal, to induce hepatic stress, as described in past work (Roldán-Alzate et al., 2015). After imaging, data were reconstructed to 14 time frames per cardiac cycle. Phase offsets were corrected automatically during reconstruction using 2nd order polynomial fitting of background tissue segmented based on thresholding of an angiogram (Walker et al., 1993; Bernstein et al., 1998). Velocity-weighted angiograms were calculated from the final velocity and magnitude data for all 14 time frames to check for variability across the cardiac cycle. However, as established in literature, hepatic flow profile typically show little variation in time (Middleton et al., 2004). Liver vasculature was segmented from PC angiograms using MIMICS (Materialise, Leuven, Belgium) by selecting a threshold level to delineate the fluid boundaries (Fig. 1). After segmentation, Ensight (CEI, Apex, NC) was used to place cut-planes manually in the splenic vein (SV), superior mesenteric vein (SMV), and the left (LPV), right (RPV), and main portal veins (PV), where flow measurements were made from 4D flow MRI data (Roldán-Alzate et al., 2013).

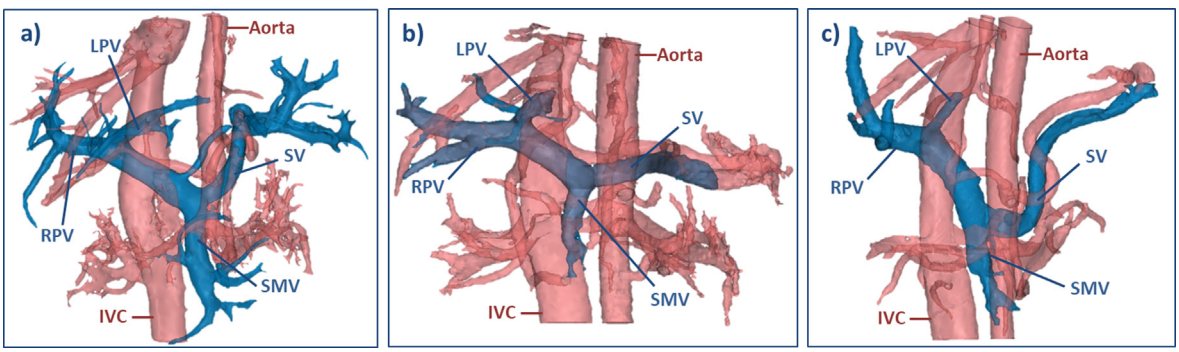

Fig. 1. MRI data was used to create three-dimensional representations of the vascular anatomy of three live liver donors. The aorta, inferior vena cava (IVC), left portal vein (LPV), right portal vein (RPV), splenic vein (SV), and superior mesenteric vein (SMV) are labeled for (a) donor 1, (b) donor 2, and (c) donor 3.

Virtual Surgery for Portal Confluence: The segmented vasculature of each liver donor subject (3 subject-specific anatomies in total) was used to create a model representing the portal vein, including the SMC and the right and left portal branches (Fig. 2a–c). The models were then imported into 3-matic (Materialise, Leuven, Belgium), where they were virtually modified to cre-

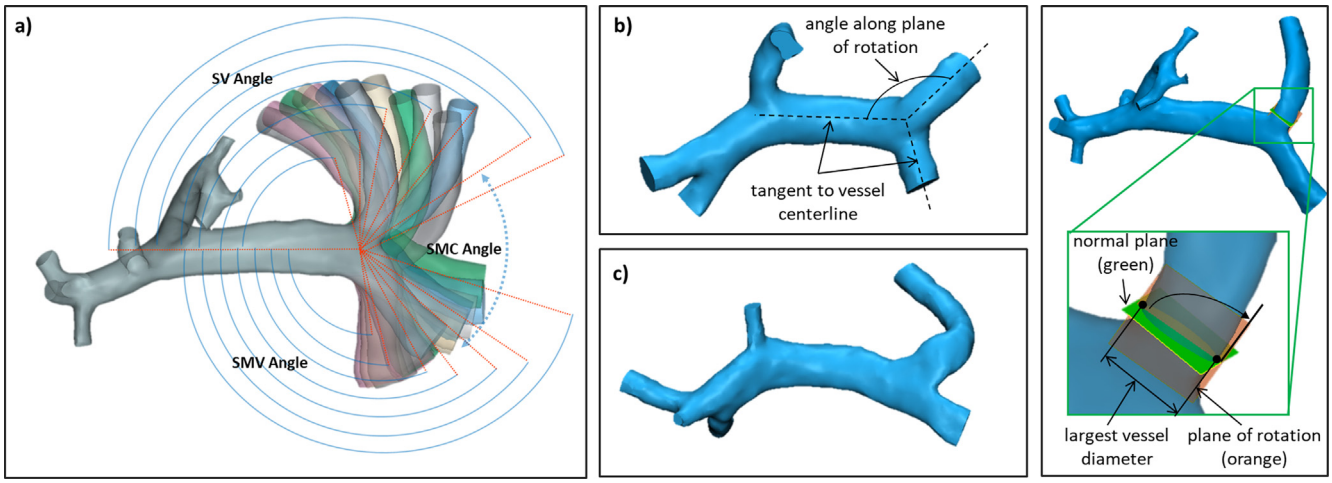

Fig. 2. Three-dimensional models were created from the segmented vasculature of (a) donor 1, (b) donor 2, and (c) donor 3 for computational simulation. The vessel angles of each model was modified, as shown on the donor 1 model in (d), to create a variety of SMC configurations. Each angle was modified by first cutting the contributing vessel normal to the flow path (green plane in (d)), and then finding the largest vessel diameter to rotate through a plane that is normal to the normal plane (orange plane in (d)). (For interpretation of the references to color in this figure legend, the reader is referred to the web version of this article.)

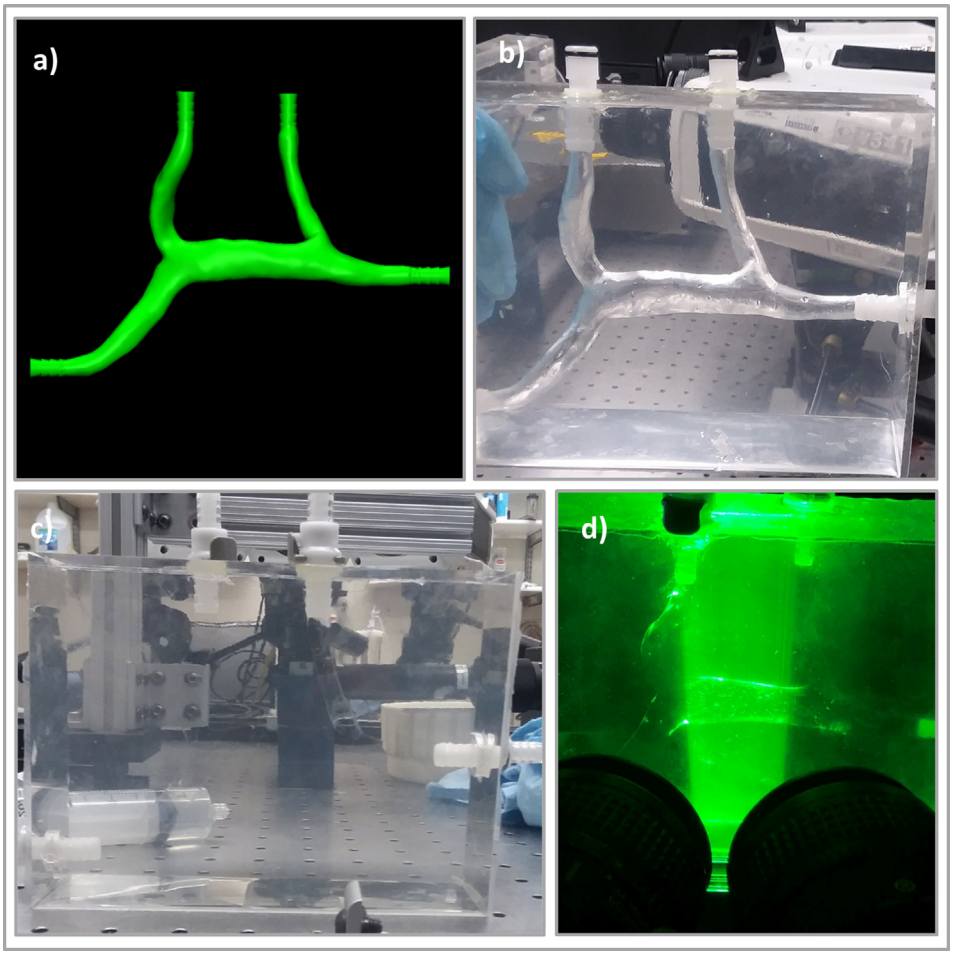

Fig. 3. Vessel anatomy from donor 1 was used to create (a) an experimental portal vein model by 3D printing the vessel flow path and dissolving it from a silicone block (b). To perform particle image velocimetry experiments, the index of refraction of the experimental fluid was matched to index of the silicone block (c). The model was then illuminated with a laser light sheet so that fluid particle motion could be tracked throughout the model (d).

ate a variety of SMC configurations. To do this, a flow path centerline was generated through the main portal vein, the SV, and the SMV based on the velocity information from 4D MRI data. The two vessels contributing to the SMC, the SV and SMV, were then cut at an orientation normal to the flow path centerline. The length of largest diameter of both the SV and SMV was determined, and a virtual plane was placed through this axis, normal to the "normal" plane (see Fig. 2d). This was termed the "plane of rotation." The SV and SMV vessels were then detached from the portal vein and rotated along the plane of rotation to achieve the desired angle with the main portal vein flow path, and then re-attached to the portal vein. Aligning the plane of rotation along the length of largest vessel diameter minimized any torsional geometry that may result from vessel segment rotation. This process was repeated to create 16–17 confluence orientations for each of the 3 donor vasculature models, resulting in 53 total vascular model iterations. The angle between the splenic vein and main portal vein was defined as the SV Angle; the angle between the superior mesenteric vein and the main portal vein was named the SMV angle; and the angle between the splenic vein and superior mesenteric vein was denoted as the SMC angle. These angles were measured between points that were tangent to the vessel segment centerline and along the plane of rotation (Fig. 2b). A representation of these parameters is shown in Fig. 2a, and examples of the models created for subjects 2 and 3 are shown in Fig. 2b and c, respectively. For analysis purposes, the variation types of each model were separated into four groups. Group 1 consisted of models with modified SV and SMV branch angles, Group 2 consisted of models with only SV angle variation, Group 3 included models with solely SMV angle variation, and Group 4 included models with total confluence angle variation (the angle between SV and SMV remained unchanged, but angle of the SMC relative to the main PV changed). The vessel orientation angles are recorded for each model in data supplement.

Computational Fluid Dynamics Simulations: Each virtually modified model was prepared for simulation by creating a computational mesh in ICEM (Ansys, Inc. Cannonburg, PA, USA). The mesh of each model was then imported into Fluent (Ansys, Inc Cannonburg, PA, USA), where steady blood flow simulations were performed with a fluid density of 1060 kg/m^3 and viscosity of 0.0035 kg/m s. Inlet flow conditions were set for the SV and SMV inlets, whose values were obtained from the in vivo 4D flow MRI quantification. This included an inflow rate of 412 ml/min at the SV and an inflow rate of 592 ml/min at the SMV. These inlet flow rates were kept constant through all model iterations so as to minimize confounding factors in the geometric analysis. Outflow percentages were also set for each outlet boundary as 83% of total outflow through the right portal vein and 17% of total flow through the left portal vein branch. These percentages were derived from the 4D MRI flow quantification for each subject, and they represent the flow patterns that develop due to the hepatic resistance to flow in downstream vasculature. These were also kept constant across simulations, so that flow inlet-specific flow split to the right and left lobe of the liver could be analyzed without the confounding factor of varying total flow. Fluid structure interaction was not considered due to minimal pulsatile motion in portal circulation (Middleton et al., 2004).

Validation Model: A physical model was created for validation of the flow structures that can develop in portal vein geometries. To create a representative model, a 3D geometry was produced from the flow path of the donor 1 portal vein anatomy (Fig. 3a). The model was then 3D-printed (Ultimaker 3 Extended, Ultimaker B.V. Cambridge, MA) using a dissolvable polyvinyl acid material. Silicone elastomer was poured around the model and allowed to cure. When the elastomer had cured, the 3D-printed anatomy was dissolved with water, leaving a void for the portal venous flow path (Fig. 3b). After fixing connectors to each portal branch opening, the model was connected to a positive displacement pulsatile pump in line with a hemodynamic conditioning head (BDC PD-1100, BDC Laboratories, Wheat Ridge, CO). In order to attain a more realistic steady hepatic flow, a compliance chamber and long sections tubing were used to dampen the pulse of the inlet flow waveform.

Tomographic particle image velocimetry (tomo-PIV) experiments were performed on the portal vein model using a Flowmaster PIV system (LaVision, Göttingen, Germany) with a dual-pulse 527 nm Nd:YLF laser (Photonics Industries International, Inc., Long Island, NY) and three high-speed cameras (Phantom v341, Vision Research, Wayne, NJ). To match the index of refraction of the silicone portal vein model, a glycerol-water mixture was used as the experimental fluid (density of 1113.5 kg/m^3 and viscosity of 0.0045 kg/m s). After the index of refraction was matched (Fig. 3c), double-frame images were recorded during laser illumination (Fig. 3d) at a frame rate of 402 Hz, with time separation of 230 μs for a maximum fluid particle displacement of 152 μm. A total of 600 sets of images, resulting in 1.5 s of acquisition time, were acquired to ensure the inclusion of a complete cardiac cycle (1 s). The images were pre-processed using subtraction of a mean intensity image and Gaussian smoothing (3×3) to eliminate errors caused by small differences in refractive index. The resulting spatial resolution for the tomo-PIV experiment was $0.14 \times 0.14 \times 0.14$ mm. A separate PIV-based CFD simulation, with water-glycerol inputs as described above, was run to see if the type of patterns that CFD was producing in these portal models was representative of realistic flow.

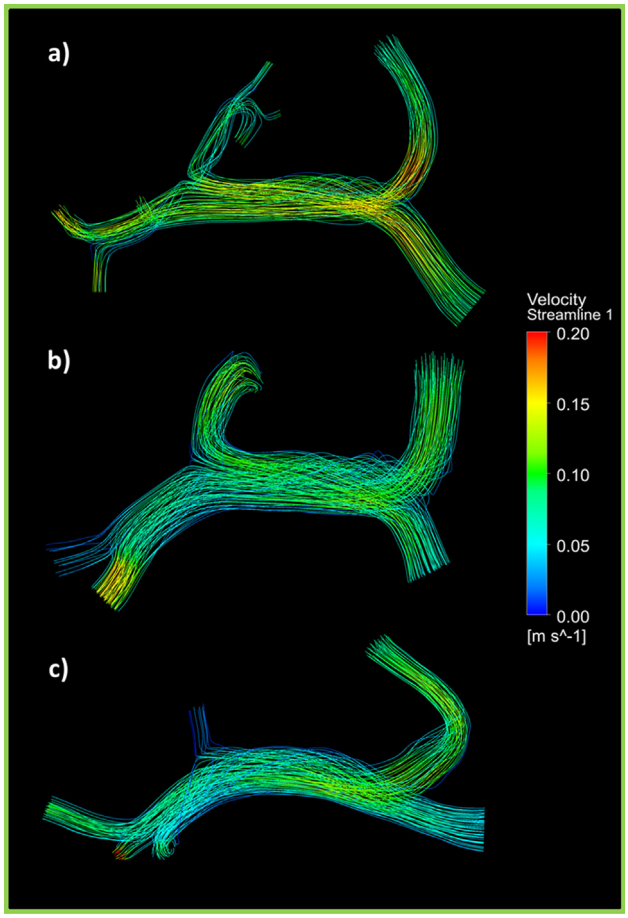

Fig. 4. 4D Flow MRI data was used to create velocity streamline representations through select computational models of (a) donor 1, (b) donor 2, and (c) donor 3.

Data analysis: *Streamlines and Flow Distribution:* The blood flow results from computational simulation, in-vivo imaging, and PIV were imported into Ensight (CEI, Apex, NC) for further analysis. Blood velocity streamlines were generated throughout the portal system from the splenic vein and superior mesenteric vein as visualized in Figs. 4–7. 150 streamlines seed points were emitted from each inlet. The number of streamlines that traveled through the right and left portal vein branches were quantified based on whether they originated in the SV or SMV. Note that flow was steady in these cases. Therefore, the streamlines are representative of the blood particle pathlines in the results of this work. To test for robustness of this flow distribution analysis, a small repeated seeding study was performed. For this robustness study, one portal vein model was run with 8 different inlet seeding densities (uniform across the inlets), ranging from 25 to 200 seeding points per inlet. Results (included in the data supplement) displayed a 2–4% deviation in outlet flow percentage across the varied-seeding models.

Vorticity and Helicity: The amount of flow rotation, and potentially mixing, can be represented in part by metrics of vorticity and helicity. *Vorticity* represents the magnitude of the three components of flow rotation,

$$\omega_x = \frac{\partial w}{\partial y} - \frac{\partial v}{\partial z} \quad \omega_y = \frac{\partial u}{\partial z} - \frac{\partial w}{\partial x} \quad \omega_z = \frac{\partial v}{\partial x} - \frac{\partial u}{\partial y}$$

where ω represents vorticity and u, v, and w represent the velocities in the x, y, and z coordinate directions, respectively. *Helicity* is indicative of the rotation of the fluid and the fluid momentum, and is calculated by the equation

$$H = v \cdot \omega$$

where v is the blood velocity and ω is overall vorticity. In an attempt to quantify the differences in the helical flow patterns between models and subject groups, the vorticity and helicity were calculated from the simulation and subject imaging velocity data in Ensight (CEI, Apex, NC). Helicity was measured in the "confluence volume" by segmenting the region of the portal vein that lies between the SMC and distal bifurcation and then imposing the volume in Ensight to measure the helicity in this region. Vorticity was

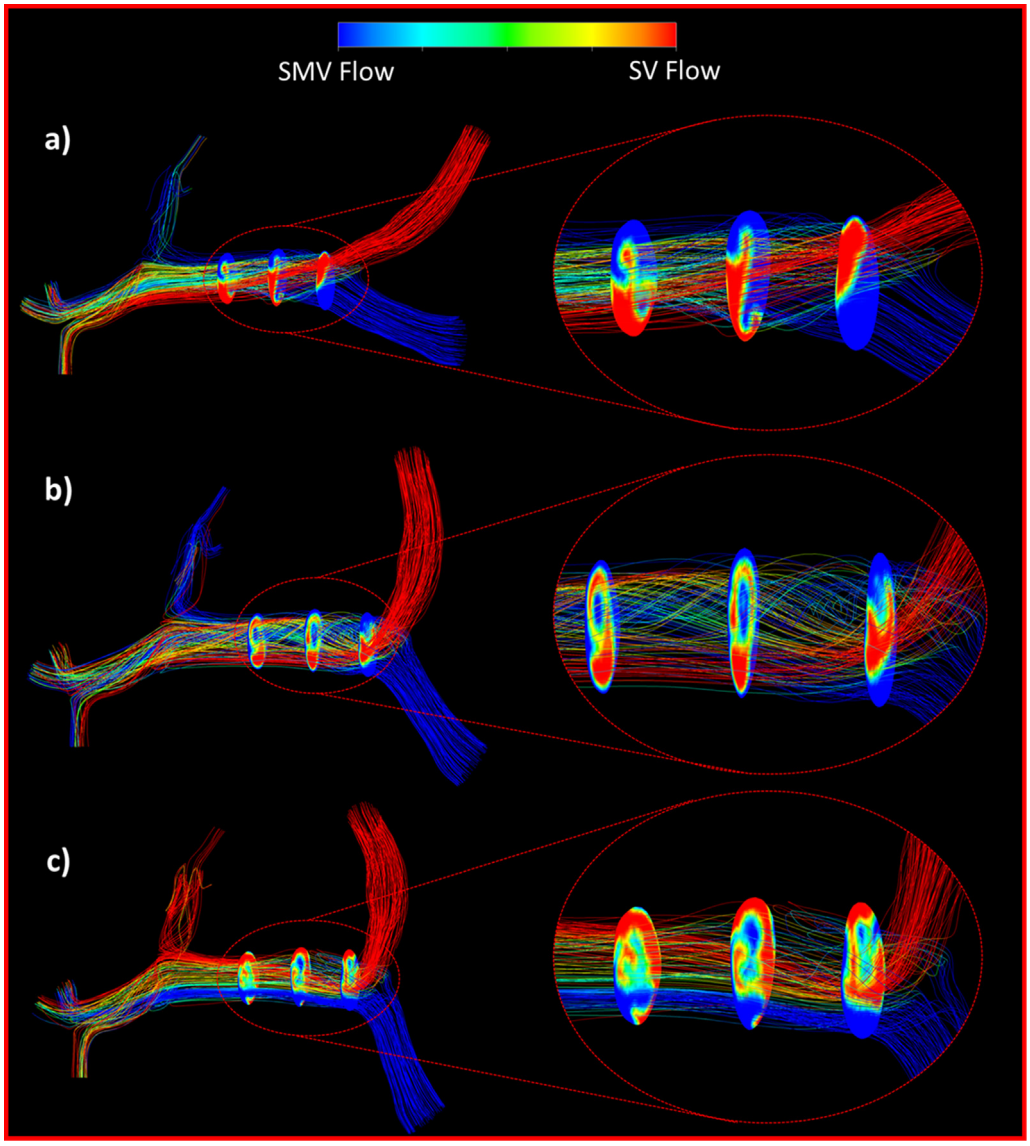

Fig. 5. Velocity streamlines were generated from the splenic vein (SV) and superior mesenteric vein (SMV) to visualize helical flow structure formation (circled in red) and blood flow distribution throughout the portal vasculature of three geometric iterations of donor 1 vasculature. (For interpretation of the references to color in this figure legend, the reader is referred to the web version of this article.)

measured in cut planes placed at locations throughout the main portal vein. The helical pattern of the flow distal to the portal confluence was also visually compared between computational models, human subject data, and the validation model through observation of streamlines through the main portal vein, as seen in Figs. 5 and 6.

Dynamic pressure: The term "dynamic pressure" was used to indicate the energy per unit volume of fluid. This was calculated during post processing in Ensight. This gives an indication of the pressure involved with fluid motion and flow distribution changes. Total pressure (static + dynamic) was not reported, as invasive measurements would be needed. Dynamic pressure was measured throughout the whole model volume. Dynamic pressure gradients, or differences, between the various locations were measured to get a representation of the dynamic pressure drop.

Statistical Analysis: To examine the relationships among SV, SMV, and PV branch angles, flow distribution, dynamic pressure, vorticity, and helicity, linear regression analyses and a Student's paired *t*-test were conducted. The correlation coefficient, r, was used to represent the strength and direction of a linear relationship between two variables. A p-value less than 0.05 indicated statistical significance. For the healthy vs. cirrhosis subject comparison, both pre- and post- meal data was compared. However, due to the amount of data and limited space, only significant results were presented. Given that analyses were based on random biological flows that also adhere to the governing equations of fluid flow, a Gaussian distribution was assumed for statistical analysis.

3. Results

Correlation relationships between measured hemodynamic metrics for in-vivo data are summarized in Table 1. In fasting healthy subjects, the proportion of flow from the SV to the left lobe of the liver decreased with increasing confluence angle. However, this trend did not appear in healthy subjects after a meal (Fig. 7).

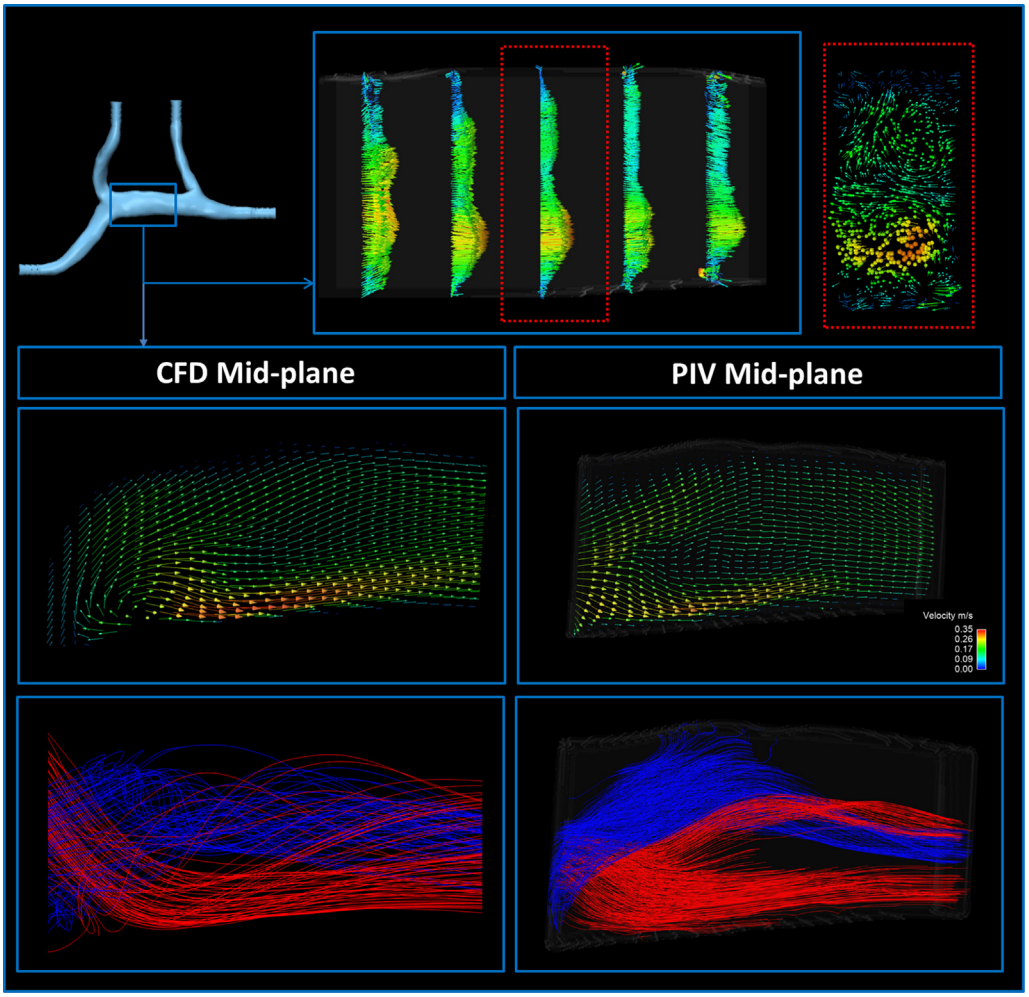

Fig. 6. Velocity vectors and inlet-specific streamlines in representative cut planes of the portal vein model obtained with particle image velocimetry and computational fluid dynamics.

Table 1
Linear regression results for in-vivo geometric and hemodynamic variable relationships with strong correlation.

Group	Dependent variable	Independent variable	Correlation coefficient	p-value
Healthy	Flow from SV to Left Lobe	Confluence angle	−0.95	0.004
Patient	Vorticity	Confluence angle	−0.8	0.06
Patient	Flow from SMV to Left lobe	Helicity	−0.75	0.14
Patient	Helicity	Confluence angle	−0.72	0.1
Patient	Kinetic energy	Confluence angle	−0.71	0.11

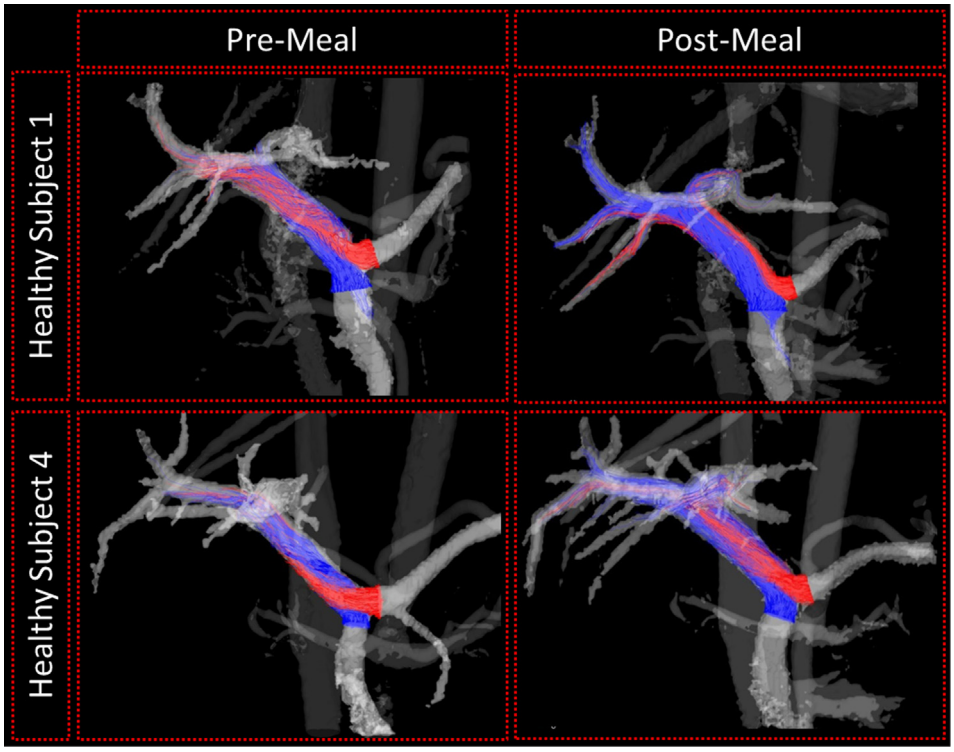

Fig. 7. Velocity streamlines can be observed following the confluence of the SV (Red) and SMV (Blue) from in to vivo imaging data in healthy subjects. Patterns of these streamlines may be indicative of mixing and blood flow distribution in distal vasculature. (For interpretation of the references to color in this figure legend, the reader is referred to the web version of this article.)

Further, these trends were not present in the cirrhotic patients. Vorticity, helicity, and kinetic energy all decreased with increasing confluence angle in patients, but not in healthy subjects. Helicity and vorticity were non-significantly higher in patients than in healthy subjects ($p = 0.12$, $p = 0.09$) (Fig. 8).

The velocity streamlines through representative computational models of each donor anatomy are shown in Fig. 4 and flow distribution streamlines, along with helical structure visualizations, are displayed in Fig. 5. Table 2 details the significant linear regression results for the computational models. In at least one group from each donor, helicity was strongly correlated with SMC angle. However, the direction of this correlation depended on the angle configuration type. Additionally, the flow distribution between the right and left portal venous branches were significantly correlated to helicity in some of the models and configurations. For model 1, more SV flow tended to go to the LPV branch as helicity increased, but this flow decreased with increasing helicity in models 2 and 3. The flow distribution was also moderately correlated to SMC angle. When SMC angle was increased, the percentage of flow to the LPV from the SV inlet increased, and the amount of flow traveling from the SMV to the LPV tended to decrease. Lastly, average dynamic portal pressure was strongly correlated to branch angle magnitudes. In model 1, there was a strong positive correlation between dynamic pressure gradient and SV angle ($r = 0.738875$, $p = 0.01$). In model 2, there was a strong negative correlation between dynamic portal pressure and SMV angle ($r = 0.87$, $p = 0.005$). In model 3, a strong negative correlation was observed between dynamic pressure and SV angle ($r = 0.82$, $p = 0.001$), and a strong positive correlation was seen between dynamics pressure and SMV angle ($r = 0.68$, $p = 0.01$).

Velocity field results from the particle image velocimetry experiment are shown on cut planes throughout the portal vein model in Fig. 6. As in the CFD models, vortex formation was observed on cut planes through representative velocity vectors. Helical flow patterns were also observed through the development of swirling throughout the model.

4. Discussion

Hepatic hemodynamic metrics are used to understand normal blood flow patterns in healthy circulation and abnormal patterns in states of disease and hepatic vasculature modification. This is particularly prevalent when considering the development and function of the portal helix, a pattern characterized by a swirling flow path often found following the spleno-mesenteric confluence. The presence and absence of this pattern has been studied as it pertains to health and disease, but its effects on downstream hepatic function have yet to be determined. In this study, we analyzed the effects of the portal helix on hemodynamic metrics and blood flow distributions, and examined the influence of SMC angle orientation on flow distribution and helical structure development.

Through computational analysis of three portal venous models in a variety of configurations, it was observed that the degree of portal helix formation can be significantly correlated with SMC orientation in a variety of portal vein configurations. Furthermore, computational results displayed significant correlations between SMC orientation, flow distribution, and dynamic pressure gradients. Through in-vivo analysis, it was also observed that the geometry of the SMC significantly affected the lobe-specific portal flow distribution in healthy subjects before a meal, although non-significant post-meal trends were also observed. Furthermore, through the larger amount of significant data relationships in cirrhotic patients than in healthy subjects seen in Table 1, and the stronger correlations among cirrhotic patients in Fig. 8, we detected greater helical flow magnitudes, and more flow distribution dependence on helix formation, in patients with cirrhosis than was observed in healthy subjects. As a result, we hypothesize that

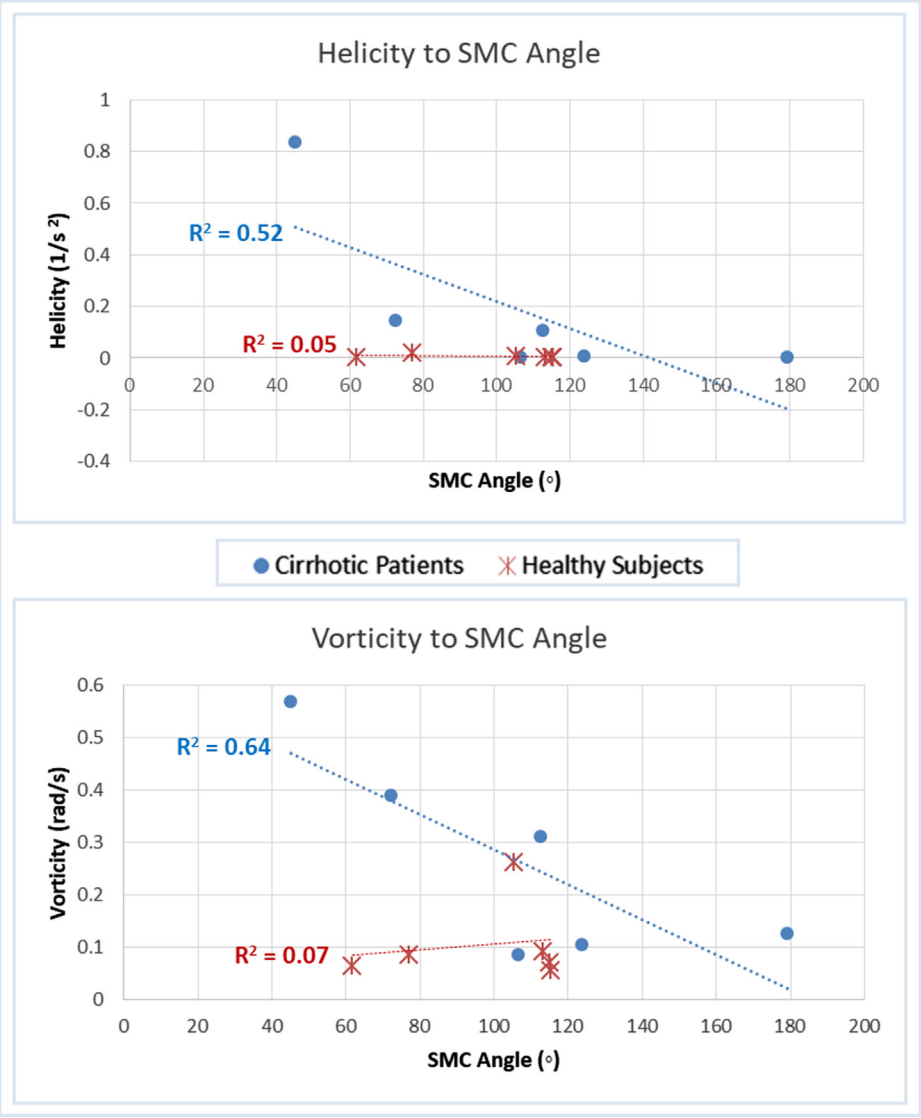

Fig. 8. The development of vortices and helical flow patterns and their relationship to SMC angle varied between healthy subjects and patients with cirrhosis. Pre-meal data is shown.

Table 2
Linear regression results for computational geometric and hemodynamic variable relationships with strong correlation and statistical significance.

Variable relationship	Model group	Correlation coefficient	p-value
Donor 1			
Helicity to SMC Angle	1	0.81	0.05
	2	0.92	0.03
	4	−0.91	0.03
SV Flow Percentage through LPA to SMC Angle	3	0.89	0.05
Donor 2			
Helicity to SMC Angle	2	0.91	0.04
SMV Flow Percentage through LPA to Helicity	3	0.98	0.02
SV Flow Percentage through LPA to SMC Angle	3	−0.93	0.01
SV Flow Percentage through LPA to SV Angle	4	0.97	0.01
Donor 3			
Helicity to SMC Angle	1	0.93	0.02
SMV Flow Percentage through LPA to Helicity	3	0.89	0.05

both the degree of helix formation and confluence vessel orientation significantly affect downstream portal hemodynamics. However, it is important to note that the direction of correlation relationships between SMC angle and hemodynamic metrics varied among different computational model configuration types and human subjects. Therefore, although significant relationships

between parameters have been observed, there are clearly other factors involved that must be studied to get a clearer picture of what governs these fluid dynamic and geometric relationships. With further study, the physiological implications of these fluid dynamic and geometric relationships downstream of the SMC may be better understood. For example, when blood from the SV and SMV is not mixed or separated properly, then mal-distribution to the right and left lobes of the liver can occur. Due to the fact that blood composition of flow from the SV and SMV is not homogenous, mal-distribution can have detrimental effects on lobe-specific liver health. Furthermore, the dynamic portal pressure variations may have negative implications on liver perfusion. When dynamic pressure is altered, significant changes in upstream and downstream flow patterns will result, potentially leading to an increase or decrease in perfusion rate.

A limitation of past work on hepatic flow is the reliance on imaging and simulation flow data for intricate flow patterns analysis. The spatial resolution of MR imaging may not be adequate to examine the finest details of flow structures. Additionally, computational simulation provides only "computed" patterns that are highly dependent on boundary conditions. To further work towards a validation model of the fluid dynamic results produced with these methods, real fluid flow analysis with particle image velocimetry was implemented. Through this analysis, we found similar development of vortices and helical flow structures throughout the portal vein model. Although similar flow patterns were observed through this experimental geometry, future studies will still be needed to improve the patient-specificity of such experimental models so that direct quantitative comparisons can be made with experimental results.

There are some limitations to this study that warrant discussion. First of all, only three patient-specific geometries were used for the computational study. The rest of the models that were used for computational analysis were derived from these patient-specific geometries. Consequently, these additional models do not themselves replicate exact in-vivo anatomy, but only potential geometric configurations. This may have limited the implementation of potential confounding geometric and fluid flow factors that exist in-vivo. Therefore, to examine the applicability of the phenomena observed through this study, we looked at portal helix effects in two in-vivo patient data sets. Yet, due to a small sample size, the clinical relevance may still be limited Lastly, there are still a number of current limitations on patient-specific particle image velocimetry. Although similar flow patterns can be produced in the experimental model as seen in-vivo, exact comparison of in-vivo and PIV data is limited by the ability to replicate in-vivo conditions other than the geometry itself. Furthermore, quantitative comparisons of the full portal vessel volume are a challenge with the current experimental setup. Although we obtained volumetric data with tomo-PIV, the volume of the portal vein is larger than the volume that we can analyze with our PIV setup. Therefore, volume measurements of helicity and flow distribution could not be appropriately compared with our full-volume CFD data. Future work will continue to improve on this patient-specificity and employ a greater number of experimental models so that comparison statistics can be calculated.

5. Conclusion

Using a combination of 4D flow MRI, computational simulations, and particle image velocimetry, we found significant relationships between portal vessel geometry, flow structure development, and blood flow distribution in distal hepatic vasculature. With further development and application in other vascular territories, the methods of this study may be used to inform clinical analysis and planning tools.

Acknowledgements

The research presented was supported by the NIH (UL1TR000427, TL1TR000429). The content is solely the responsibility of the authors and does not necessarily represent the official views of the National Institutes of Health. The authors also wish to acknowledge support from GE Healthcare who provides research support to the University of Wisconsin.

Conflict of interest statement

The authors have no conflict of interest to state.

Appendix A. Supplementary material

Supplementary data to this article can be found online at https://doi.org/10.1016/j.jbiomech.2019.03.025.

References

Bernstein, M.A., Zhou, X.J., Polzin, J.A., King, K.F., Ganin, A., Pelc, N.J., Glover, G.H., 1998. Concomitant gradient terms in phase contrast MR: analysis and correction. Magn. Reson. Med. 39, 300–308.
Cohn, J.N., Khatri, I.M., Groszmann, R.J., Kotelanski, B., 1972. Hepatic blood flow in alcoholic liver disease measured by an indicator dilution technic. Am. J. Med. 53, 704–714.
Ho, H., Sorrell, K., Bartlett, A., Hunter, P., 2012. Blood flow simulation for the liver after a virtual right lobe hepatectomy. Med. Image Comput. Comput. Assist. Interv. 15, 525–532.
Johnson, K.M., Lum, D.P., Turski, P.A., Block, W.F., Mistretta, C.A., Wieben, O., 2008. Improved 3D phase contrast MRI with off-resonance corrected dual echo VIPR. Magn. Reson. Med. 60, 1329–1336.
Lara, M., Chen, C.Y., Mannor, P., Dur, O., Menon, P.G., Yoganathan, A.P., Pekkan, K., 2011. Hemodynamics of the hepatic venous three-vessel confluences using particle image velocimetry. Ann. Biomed. Eng. 39, 2398–2416.
Middleton, W.D., Kurtz, A.B., Hertzberg, B.S., 2004. Ultrasound: The Requisites. Mosby, St. Louis, MO.
Ralls, P.W., 1990. Color Doppler sonography of the hepatic artery and portal venous system. AJR Am. J. Roentgenol. 155, 517–525.
Richardson, P.D., Withrington, P.G., 1981. Liver blood flow. I. Intrinsic and nervous control of liver blood flow. Gastroenterology 81, 159–173.
Roldán-Alzate, A., Francois, C.J., Wieben, O., Reeder, S.B., 2016. Emerging applications of abdominal 4D flow MRI. AJR Am. J. Roentgenol. 207, 58–66.
Roldán-Alzate, A., Frydrychowicz, A., Niespodzany, E., Landgraf, B.R., Johnson, K.M., Wieben, O., Reeder, S.B., 2013. In vivo validation of 4D flow MRI for assessing the hemodynamics of portal hypertension. J. Magn. Reson. Imaging 37, 1100–1108.
Roldán-Alzate, A., Frydrychowicz, A., Said, A., Johnson, K.M., Francois, C.J., Wieben, O., Reeder, S.B., 2015. Impaired regulation of portal venous flow in response to a meal challenge as quantified by 4D flow MRI. J. Magn. Reson. Imaging 42, 1009–1017.
Rosenthal, S.J., Harrison, L.A., Baxter, K.G., Wetzel, L.H., Cox, G.G., Batnitzky, S., 1995. Doppler US of helical flow in the portal vein. Radiographics 15, 1103–1111.
Rutkowski, D.R., Reeder, S.B., Fernandez, L.A., Roldán-Alzate, A., 2017. Surgical planning for living donor liver transplant using 4D flow MRI, computational fluid dynamics and in vitro experiments. Comput. Methods Biomech. Biomed. Eng.: Imaging Visual., 1–11
Scheinfeld, M.H., Bilali, A., Koenigsberg, M., 2009. Understanding the spectral Doppler waveform of the hepatic veins in health and disease. Radiographics 29, 2081–2098.
Sugimoto, H., Kaneko, T., Nakao, A., 2002. Poststenotic dilatation and helical flow in the umbilical portion of the portal vein. J. Hepatol. 36, 704.
Van As, A.B., Hickman, R., Engelbrecht, G.H., Makan, P., Duminy, F., Kahn, D., 2001. Significance of the portal vein helix. S Afr. J. Surg. 39, 50–52.
Walker, P.G., Cranney, G.B., Scheidegger, M.B., Waseleski, G., Pohost, G.M., Yoganathan, A.P., 1993. Semiautomated method for noise reduction and background phase error correction in MR phase velocity data. J. Magn. Reson. Imaging 3, 521–530.
Zhang, L., Yin, J., Duan, Y., Yang, Y., Yuan, L., Cao, T., 2011. Assessment of intrahepatic blood flow by Doppler ultrasonography: relationship between the hepatic vein, portal vein, hepatic artery and portal pressure measured intraoperatively in patients with portal hypertension. BMC Gastroenterol. 11, 84.